ChemComm

COMMUNICATION

View Article Online
View Journal

Cite this: DOI: 10.1039/c5cc03895b

Received 11th May 2015,
Accepted 7th July 2015

DOI: 10.1039/c5cc03895b

www.rsc.org/chemcomm

A contamination-insensitive probe for imaging specific biomolecules by secondary ion mass spectrometry†

Selda Kabatas,‡[a] Ingrid C. Vreja,‡[bc] Sinem K. Saka,[b] Carmen Höschen,[d] Katharina Kröhnert,[b] Felipe Opazo,[b] Silvio O. Rizzoli*[be] and Ulf Diederichsen*[ae]

Imaging techniques should differentiate between specific signals, from the biomolecules of interest, and non-specific signals, from the background. We present a probe containing ^{15}N and ^{14}N isotopes in approximately equal proportion, for secondary ion mass spectrometry imaging. This probe designed for a precise biomolecule analysis is insensitive to background signals.

The identification of specific elements in biological imaging typically relies on their coupling to tags that are not naturally present in cellular preparations. These tags include fluorophores in fluorescence microscopy, gold particles in immunoelectron microscopy, or enzymes in immunohistochemistry. This approach enables the analysis with high contrast, but is disturbed by the presence of any contaminations in the preparations. The contaminations are any of the elements from the background that produce signals similar to those of the tags. In fluorescence imaging, the best-known source of contaminating signals is the non-specific autofluorescence of cellular elements. Similarly, the presence of naturally occurring electron-dense particles, and the activity of native enzymes, can cause problems in electron microscopy and immunohistochemistry, respectively.[1]

To avoid this issue we developed a novel type of tag, composed of elements that occur naturally in the preparation, but artificially manipulated to achieve different proportions to the native ones. This type of tag implies the analysis of at least two elements, in order to determine their ratio. This is possible using mass spectrometry, especially secondary ion mass spectrometry, SIMS, in which multiple isotopes emerging from the sample are measured simultaneously.

Some isotopes are common in biological samples, such as ^{14}N or ^{12}C, while others have far lower abundances, including ^{15}N (natural abundance ratio of 0.00367, meaning 0.367% of all N isotopes) and ^{13}C (natural abundance ratio of 0.012).[2] This opens the possibility of generating biomolecule tags enriched in low-abundance isotopes. A probe containing a high number of ^{15}N isotopes will increase the proportion of this isotope at specific sites in the preparation, where the particular biomolecules are located. This constitutes a signal that will be visible in $^{15}N/^{14}N$ ratio images. This signal will not be sensitive to contamination with any type of N-containing material, neither biological, nor artificial (embedding material, fixatives). Any contaminant would contain the same ratio of $^{15}N/^{14}N$ as the biological preparation (0.00367), thus leaving unaffected the ratio increase caused by the probe.

To implement this approach we turned to nanoscale secondary ion mass spectrometry (NanoSIMS) imaging, which reaches a resolution comparable to that of fluorescence microscopy in the lateral plane, and even higher in the axial direction.[3,4] The difficulty of this type of technology has been to provide tags that detect specifically a biomolecule of interest. We have recently taken advantage of the flexibility of genetic code expansion[5–7] to generate an isotopic probe for NanoSIMS, based on ^{19}F isotopes.[8] The low ^{19}F abundance in biological preparations enables its identification as a label using NanoSIMS with a relatively high contrast, just as fluorophores help to identify the protein in fluorescence microscopy. However, in a similar manner to fluorescence imaging, this procedure is highly sensitive to any ^{19}F contamination in the preparation.

To overcome this problem, we decided to use genetic code expansion followed by chemoselective labelling to introduce a probe containing a high $^{15}N/^{14}N$ ratio into specific proteins (Scheme 1). Genetic code expansion relies on the incorporation

[a] Institute of Organic and Biomolecular Chemistry, University of Göttingen, Tammannstr. 2, D-37077 Göttingen, Germany. E-mail: udieder@gwdg.de
[b] Department of Neuro- and Sensory Physiology, University Medical Centre Göttingen, Humboldtallee 23, D-37073 Göttingen, Germany. E-mail: srizzol@gwdg.de
[c] International Max Planck Research School Molecular Biology, Göttingen, Germany
[d] Department of Ecology and Ecosystem Management, Centre of Life and Food Sciences Weihenstephan, Technische Universität München, Emil-Ramann-Straße 2, D-85354 Freising, Germany
[e] Centre for Nanoscale Microscopy and Molecular Physiology of the Brain (CNMPB), Göttingen, Germany

† Electronic supplementary information (ESI) available: Experimental details, synthetic procedures, methods employed for protein labelling and measurements. See DOI: 10.1039/c5cc03895b

‡ These authors contributed equally.

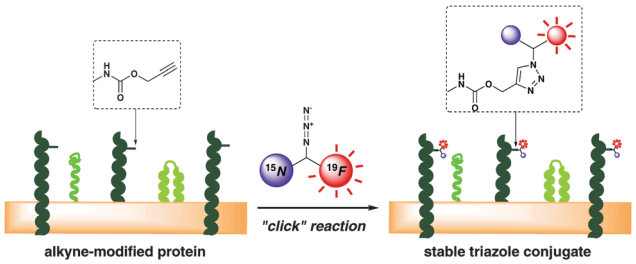

Scheme 1 Labelling of UAA-introduced proteins with a probe containing a high $^{15}N/^{14}N$ ratio and a fluorophore through azide-alkyne cycloaddition. The isotopic and fluorescent probe enables both fluorescence (confocal microscopy) and isotopic (NanoSIMS) imaging.

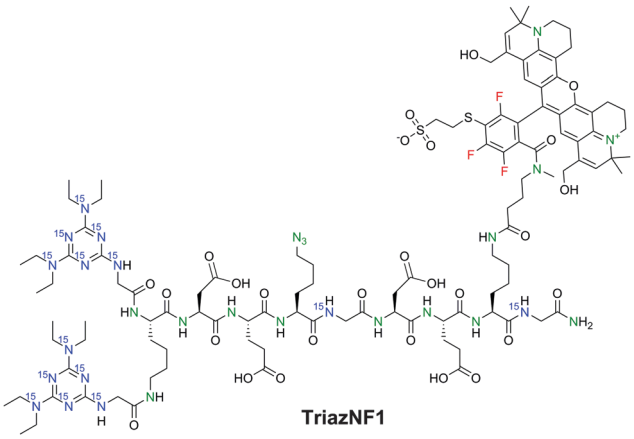

Scheme 2 The dual probe **TriazNF1** contains an azide group for click chemistry, ^{15}N (marked in blue), ^{14}N (green) and ^{19}F atoms (red) for isotopic imaging by NanoSIMS, and a Star635 fluorescent moiety for fluorescence imaging.

of an unnatural amino acid (UAA) at a defined site in a specific protein, both in prokaryotic and eukaryotic cells.[5,6] The UAA is introduced in a modified version of the protein of interest, which contains the so-called Amber stop codon (TAG).[9,10] The UAA is usually chosen to contain an azide or an alkyne moiety, which is coupled after cellular fixation to any desired probe through copper(I)-catalysed azide–alkyne Huisgen cycloaddition (click chemistry).[11–13]

To generate a suitable probe for this procedure, with a high $^{15}N/^{14}N$ ratio, we looked for small molecule candidates that contain as many ^{15}N-isotopes as possible, and whose precursor materials are commercially available with the highest possible ^{15}N-isotopic purity. We reasoned that the molecule should be easily incorporated into a peptide scaffold, preferably applying standard solid phase peptide synthesis (SPPS). Additionally, it should be non-charged under physiological conditions, to avoid hydrogen-bonding or electrostatic interactions with cell compartments during the process of protein labelling. Considering these criteria, we targeted the formation of triaminotriazine with six N-atoms.

The synthesis of the heteroaromatic compound started with the cyclization of $^{15}N_3$-biuret, a condensation product of ^{15}N-urea, to $^{15}N_3$-cyanuric acid. After conversion of $^{15}N_3$-cyanuric acid to $^{15}N_3$-cyanuric chloride, a temperature-dependent stepwise substitution of the chlorine atoms was performed yielding the bis-alkylated and glycine-modified triazine $^{15}N_6$-triazGly-OH ready for SPPS (ESI,† Section 3.1). In order to specifically label proteins, three differently charged peptides were evaluated: neutral, positive and negative, and only the negative version showed chemoselective labelling (detailed information in the ESI,† Fig. S1). Therefore, only the negatively charged peptide termed **TriazNF1** will be further discussed. The nonapeptide **TriazNF1** contains 14 × ^{15}N and 16 × ^{14}N atoms (resulting in a $^{15}N/^{14}N$ ratio of 0.875) and provides adequate solubility under physiological conditions due to the negatively charged amino acids glutamate and aspartate (Scheme 2).

Moreover, the peptide is equipped with an azide by the introduction of azidolysine for later attachment to proteins by click chemistry. Two orthogonally protected lysines were used, where the N-terminal lysine served for the linkage of two $^{15}N_6$-triazGly-OH units, while the other lysine was available for side chain attachment with Star635-NHS to enable a direct correlation of NanoSIMS with fluorescence microscopy. Synthesis of **TriazNF1** was achieved by microwave-mediated SPPS on Sieber amide resin, applying the Fmoc synthesis protocol. Cleavage from the resin and simultaneous deprotection provided the nonapeptide $^{15}N_6$-triazG-Lys($^{15}N_6$-triazG)-Asp-Glu-Lys(N_3)-^{15}N-Gly-Asp-Glu-Lys-^{15}N-Gly-NH_2 that was coupled in solution to the Star635-NHS fluorophore (ESI,† Fig. S2). The ^{19}F-content of the second-generation label was provided from the supplied fluorophore (Star635-NHS). After final purification by HPLC, the constitutional accuracy of the label **TriazNF1** was indicated by high resolution mass spectrometry.

To test the performance of the probe in NanoSIMS, we applied **TriazNF1** to mammalian cells, whose genetic code has been expanded to incorporate the alkyne-containing UAA propargyl-L-lysine (PRK), in a similar manner to our previous report.[8]

To ease the application, we also added a fluorophore to **TriazNF1**, which also enables its use in fluorescence microscopy and correlative optical isotopic nanoscopy.[4] Since the fluorophore (Star635) also contains three ^{19}F isotopes, this furthermore allows us to compare directly the $^{15}N/^{14}N$ ratio imaging with the ^{19}F measurements.

We tested three proteins involved in membrane fusion: the transmembrane SNAREs syntaxin 1 and syntaxin 13, and the membrane-anchored SNAP-25. Their specific labelling by PRK incorporation and click reaction with fluorescent probes has already been demonstrated.[8] In the presence of PRK cells were transfected with versions of these proteins containing Amber stop codons and were then coupled to **TriazNF1** by click chemistry, followed by plastic embedding, processing to 200 nm thin sections, and visualisation using both fluorescence microscopy and NanoSIMS (Fig. 1). The NanoSIMS images show a higher $^{15}N/^{14}N$ ratio in cells that have successfully incorporated **TriazNF1**, compared to the non-transfected ones (Fig. 1A–C). The $^{15}N/^{14}N$ ratio in the transfected cells is far lower than the $^{15}N/^{14}N$ ratio of the probe because the majority of the N isotopes in the cells are native cellular isotopes containing ^{15}N in the natural proportion (0.00367).

As discussed above, we expected the imaging of $^{15}N/^{14}N$ ratios to be less sensitive to contaminating background signals

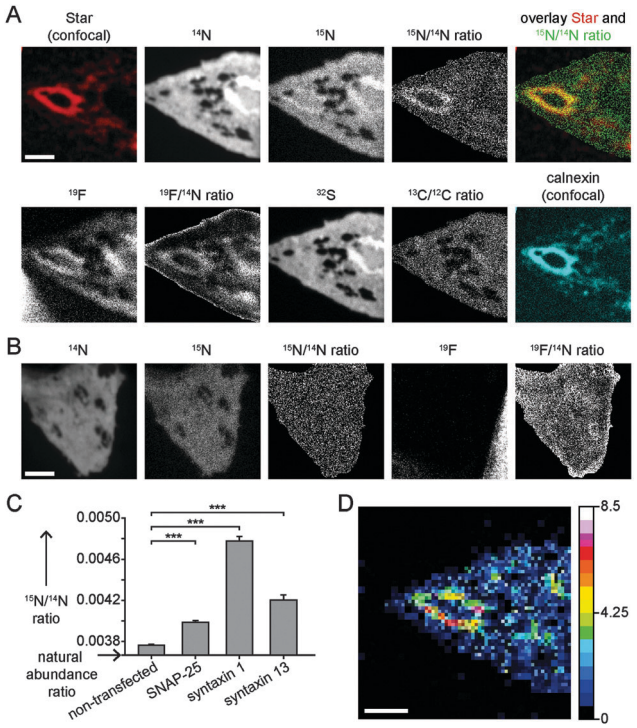

Fig. 1 **TriazNF1** specifically labeled proteins for visualisation in NanoSIMS. We incorporated PRK into syntaxin 1 while expressing it in BHK cells. We then fixed the samples and labelled them by click reaction with **TriazNF1**, followed by embedding in LR White, and thin-sectioning. (A) Representative images of a cell expressing syntaxin 1 labelled with **TriazNF1**. The top panels show the fluorescence image of **TriazNF1** (Star635 fluorescence), in confocal microscopy, and NanoSIMS images of the ^{14}N and ^{15}N isotopes, as well as their ratio. An overlay of this ratio with the fluorescence image confirms the good colocalisation of the two signals. The bottom panels show further NanoSIMS images of the same cell: ^{19}F and its ratio to ^{14}N, ^{32}S, and finally a ratio of ^{13}C to ^{12}C, as an indication of cellular turnover (based on the incorporation of L-leucine-2-^{13}C into newly secreted proteins). The ratio images only show pixels with more than 300 ^{14}N counts; lower values represent regions outside of the cell, in which the ratios are not meaningful. The last image in this row indicates the possibility of combining **TriazNF1** with immunostainings, in fluorescence microscopy (the endoplasmic reticulum protein calnexin is shown). (B) NanoSIMS measurements for a non-transfected cell. Corresponding images of the transfected and non-transfected cell are identically scaled. (C) The mean $^{15}N/^{14}N$ ratios for cells expressing different SNARE proteins are significantly higher (***, $P < 0.001$ compared to control in Student's *t*-test) than the ratio for non-transfected cells. The *Y* axis starts at the value of the natural abundance ratio (0.00367). For each condition we analysed a number of circular cellular regions of interest, of $\sim$0.123 μm^2: 15 regions for SNAP-25, 54 for syntaxin 1, 31 for syntaxin 13, and 137 for non-transfected cells. The error bars indicate the standard errors. (D) Image depicting syntaxin 1 copy number inferred from the $^{15}N/^{14}N$ ratio. Scale bar for all images, 2 μm.

than approaches based on imaging elements that are not normally present in the preparation, such as ^{19}F. This is evident in Fig. 1A, where a relatively high ^{19}F signal is visible in the nucleus of the cell. As the transmembrane protein syntaxin 1 (shown in Fig. 1A) cannot reach the nucleus, we are forced to conclude that the ^{19}F signal present here is due to a contamination with unknown fluorinated molecules in the nucleus, which, however, partly compromises the ^{19}F imaging procedure (Fig. 1A). We solved this issue partly in the past by increasing the number of ^{19}F atoms in the probe from 3 to 13,[8] which raises the signal-to-noise ratio for ^{19}F by more than four-fold. However, the use of a probe based on the $^{15}N/^{14}N$ ratio provides a much more elegant solution to the contamination problem.

TriazNF1 also enables the simple estimation of the copy number of tags measured from the preparation. While the number of tags cannot be derived from ^{19}F, due to non-specific contaminating signals, it can be derived from the isotope counts for ^{14}N and ^{15}N (ESI,† Section 5). When sufficiently large areas are measured, to compensate for the pixel-to-pixel variation in the ratio, a $^{15}N/^{14}N$ ratio close to the natural abundance (0.00367) is found for the non-transfected cells. In the presence of **TriazNF1**, the ratio increases significantly (Fig. 1C). This increase can be translated into actual copy numbers of **TriazNF1** molecules by a simple equation (ESI,† Section 5), which is based on the ^{14}N and ^{15}N counts alone. This can be estimated for each voxel, if the voxels are sufficiently large to counteract the effects of isotope counting noise. We present such an estimation in Fig. 1D, using voxels of $\sim$156 $\times$ 156 nm in the imaging plane, and a depth of $\sim$20 nm. This figure panel shows estimates, rather than exact copy numbers. The latter, however, can be obtained by calibrating the NanoSIMS instrument with standard isotopic samples, to turn the ^{14}N and ^{15}N counts into precise isotope numbers.

TriazNF1 can now be used as a label for specific proteins, and enables the investigator to analyse the composition of the organelles containing the respective proteins. For example, the cells can be treated with isotopically labelled amino acids, whose incorporation into cellular proteins gives a direct indication of cellular turnover, on the subcellular scale.[4,14–16] L-Leucine-2-^{13}C was applied for 24 h, containing one ^{13}C atom. Its incorporation into the cell can be compared with the **TriazNF1** position (Fig. 1A). In addition, the analysis of the isotopic composition of the cell is not limited to N or C isotopes. Many other organic elements can be visualised (for example ^{32}S, Fig. 1A).

Finally, the fluorophore moiety of **TriazNF1** enables the simple correlation of the isotopic images with further fluorescence images, obtained from immunostaining or other procedures (Fig. 1A, calnexin panel, in which an immunostaining for this endoplasmic reticulum marker protein is shown).

SIMS imaging is increasingly used as a technique to investigate the organisation and structure of cells and organelles.[3] The main difficulty with this and similar techniques is that, while many labels can be used to investigate, for example, the turnover of all cellular proteins, very few possibilities exist for the tagging of individual biomolecules. Some proposed methods are similar to the techniques used in fluorescence imaging and immunoelectron microscopy, coupling the protein of interest to elements that are not present in the cells, such as ^{19}F, as discussed above,[8] or lanthanide metals coupled to antibodies.[17] These probes, as seen in Fig. 1A, are inherently sensitive to contamination by ^{19}F or lanthanides in the sample. In contrast, a probe based on a change in the $^{15}N/^{14}N$ ratio, like **TriazNF1**, offers the same advantages, these being specific labelling and flexibility in both isotopic and fluorescence microscopy, while being entirely insensitive to contamination.

We would like to thank Johann Lugmeier (Department Ecology and Ecosystem Management, Centre of Life and Food

Sciences Weihenstephan, Technische Universität München, Freising-Weihenstephan, Germany) for his technical support in NanoSIMS measurements. I.C.V. acknowledges support from a Dorothea Schlözer scholarship. This work was supported by grants to S.O.R. and U.D. from the Deutsche Forschungsgemeinschaft Cluster of Excellence Nanoscale Microscopy and Molecular Physiology of the Brain (CNMPB), by grants to S.O.R. from the European Research Council (ERC-2013-CoG NeuroMolAnatomy) and DFG (SFB889/A5) and to U.D. by the DFG (SFB803/B5).

Notes and references

1 A. Denker, I. Bethani, K. Kröhnert, C. Körber, H. Horstmann, B. G. Wilhelm, S. V Barysch, T. Kuner, E. Neher and S. O. Rizzoli, *Proc. Natl. Acad. Sci. U. S. A.*, 2011, **108**, 17177.
2 G. McMahon, H. F. Saint-Cyr, C. Lechene and C. J. Unkefer, *J. Am. Soc. Mass Spectrom.*, 2006, **17**, 1181.
3 M. L. Steinhauser and C. P. Lechene, *Semin. Cell Dev. Biol.*, 2013, **24**, 661.
4 S. K. Saka, A. Vogts, K. Kröhnert, F. Hillion, S. O. Rizzoli and J. T. Wessels, *Nat. Commun.*, 2014, **5**, 3664.
5 C. C. Liu and P. G. Schultz, *Annu. Rev. Biochem.*, 2010, **79**, 413.
6 J. W. Chin, *Annu. Rev. Biochem.*, 2014, 1.
7 E. A. Lemke, *ChemBioChem*, 2014, **15**, 1691.
8 I. C. Vreja, S. Kabatas, S. K. Saka, K. Kröhnert, C. Höschen, F. Opazo, U. Diederichsen and S. O. Rizzoli, *Angew. Chem., Int. Ed.*, 2015, **54**, 5784.
9 D. R. Liu and P. G. Schultz, *Proc. Natl. Acad. Sci. U. S. A.*, 1999, **96**, 4780.
10 L. Wang, A. Brock, B. Herberich and P. G. Schultz, *Science*, 2001, **292**, 498.
11 M. Meldal and C. W. Tomøe, *Chem. Rev.*, 2008, **108**, 2952.
12 K. Lang and J. W. Chin, *ACS Chem. Biol.*, 2014, **9**, 16.
13 K. Horisawa, *Front. Physiol.*, 2014, **5**, 1.
14 D.-S. Zhang, V. Piazza, B. J. Perrin, A. K. Rzadzinska, J. C. Poczatek, M. Wang, H. M. Prosser, J. M. Ervasti, D. P. Corey and C. P. Lechene, *Nature*, 2012, **481**, 520.
15 M. L. Steinhauser, A. P. Bailey, S. E. Senyo, C. Guillermier, T. S. Perlstein, A. P. Gould, R. T. Lee and C. P. Lechene, *Nature*, 2012, **481**, 516.
16 S. E. Senyo, M. L. Steinhauser, C. L. Pizzimenti, V. K. Yang, L. Cai, M. Wang, T.-D. Wu, J.-L. Guerquin-Kern, C. P. Lechene and R. T. Lee, *Nature*, 2013, **493**, 433.
17 M. Angelo, S. C. Bendall, R. Finck, M. B. Hale, C. Hitzman, A. D. Borowsky, R. M. Levenson, J. B. Lowe, S. D. Liu, S. Zhao, Y. Natkunam and G. P. Nolan, *Nat. Med.*, 2014, **20**, 436.

